

## Dynamics of grain boundaries under applied mechanical stress

Dmitri A. Molodov · Tatiana Gorkaya ·  
Günter Gottstein

Received: 18 June 2010/Accepted: 30 December 2010/Published online: 11 January 2011  
© Springer Science+Business Media, LLC 2011

**Abstract** Recent results of experimental research into stress-induced grain boundary migration in aluminum bicrystals are reported. Boundary migration under a shear stress was observed to be coupled to a lateral translation of the grains for planar symmetrical  $\langle 100 \rangle$  tilt boundaries. This coupling proved to be the typical migration mode of any  $\langle 100 \rangle$  tilt boundary, no matter whether low- or high-angle, low  $\Sigma$  CSL coincidence or non-coincidence boundary. The measured ratios of normal boundary motion to the tangential displacement of grains are in an excellent agreement with theoretical predictions. The migration-shear coupling is also observed for asymmetrical  $\langle 100 \rangle$  boundaries. Measurements of the temperature dependence of coupled boundary migration revealed that there is a specific misorientation dependence of migration activation parameters. Grain boundaries can act during their motion under the applied stress as sources of lattice dislocations that leads to the generation and growth of new grains in the boundary region. The rate of stress-induced boundary migration decreases with increasing solute content in aluminum. Both the migration activation enthalpy and the pre-exponential mobility factor were found to increase with rising impurity concentration.

### Introduction

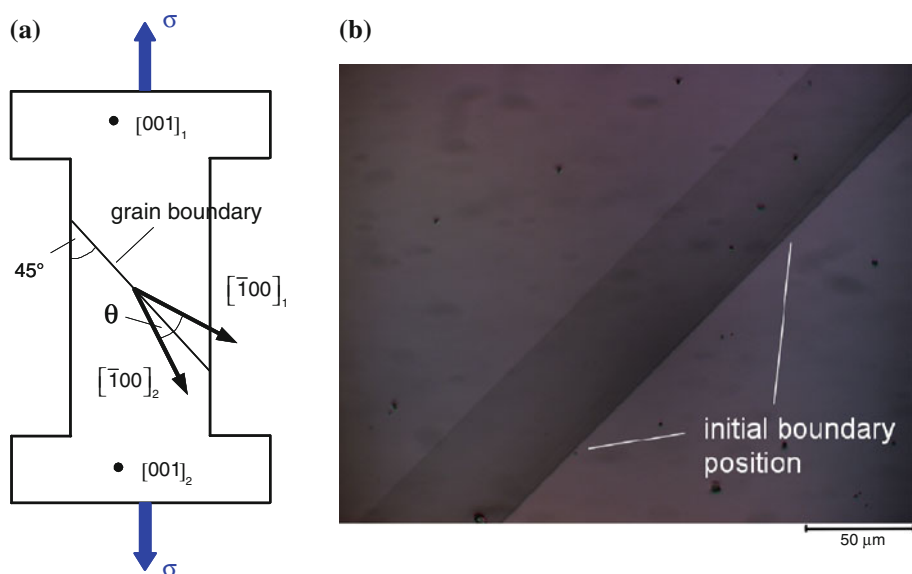
Grain boundary mediated plasticity, i.e., a shape change of a material due to grain boundary migration, is actively discussed in the literature owing to the importance of this

deformation mechanism for mechanical properties of ultra fine grained and nanocrystalline materials [1–6]. Theoretically predicted by Read and Shockley in their seminal paper on the dislocation models of grain boundaries in crystalline solids [7], stress-driven motion of symmetrical tilt grain boundaries coupled to a shear strain was first observed in experiments with low angle boundaries in Zn [8–10], which in turn furnished evidence for the dislocation character of grain boundary structure. The dislocation glide under stress causes a shear strain of the crystal region behind the moving boundary. Since at higher misorientations the grain boundary structure is no longer represented by the dislocation model, this mechanism is commonly considered to be limited to low angle tilt boundaries. However, the boundary migration-shear coupling was also observed in Zn, Al, and  $ZrO_2$  bicrystals for high angle low  $\Sigma$  coincidence tilt boundaries [11–18]. Furthermore, recently developed theoretical models [19–22] are not confined to low angle boundaries but predict the shear coupled migration of high angle boundaries as well. This has been validated in molecular dynamics computer simulations of stress driven motion of low  $\Sigma$  coincidence and non-coincidence tilt boundaries in Cu and Al [23–26].

The boundary migration accompanied by shear for random boundaries was observed by TEM investigations in nanocrystalline and ultrafine-grained polycrystals [4–6]. However, the observation of stress-affected grain boundary behavior in polycrystals cannot be interpreted unambiguously. Besides the applied stress grain boundaries experience also a curvature driving force for their displacement, which can even be affected by triple junctions. Due to their non-planar shape, different sections of the grain boundaries in polycrystals are exposed to different stress conditions that substantially complicate an analysis. Moreover, the observed grain boundaries in a polycrystalline specimen

D. A. Molodov (✉) · T. Gorkaya · G. Gottstein  
Institute of Physical Metallurgy and Metal Physics,  
RWTH Aachen University, 52056 Aachen, Germany  
e-mail: molodov@imm.rwth-aachen.de

**Fig. 1** **a** Geometry of the bicrystalline specimens for the tensile loading used in experiments; **b** Optical contrast, which appears due to the altered reflectivity of the aluminum oxide layer in the sheared crystal region behind the boundary, and traces of the initial and final position of a  $76.4^\circ\langle100\rangle$  tilt boundary on the specimen surface after 30 min annealing at  $380^\circ\text{C}$  under an applied tensile stress of 0.26 MPa



cannot be comprehensively characterized, particularly with respect to the boundary plane inclination that can be crucial for the boundary response to applied stress. Therefore, grain boundary behavior under stress is most appropriately studied on specific boundaries with exactly defined geometry in specially grown bicrystals. In situ observations in specimens with planar boundaries under a constant load and temperature provide the opportunity to measure the rate of both the normal boundary migration and the shear, to extract their relation and to determine the temperature dependence of coupled boundary migration for various boundaries in a wide range of grain boundary character.

In this article the results of experimental investigations of boundary migration coupled to shear in bicrystals with various  $\langle100\rangle$  tilt boundaries are reported.

## Specimens and applied measurement techniques

Shear stress-induced boundary motion coupled to a shear strain was measured in specimens with a cross-section of about  $4.9 \times 4.7$  mm (Fig. 1a) fabricated from specially grown Al bicrystals and subjected to a constant tensile load ranging from 5 to 20 N at different elevated temperatures. Details of crystal growth, bicrystal characterization and sample preparation are given elsewhere [27–29].

Both discontinuous and continuous methods were used for coupled boundary migration measurements. Most experiments so far were performed by utilizing a step-wise annealing technique and measuring the boundary positions prior to loading and after unloading. The boundary displacement was revealed by an optical contrast on the surface of the bicrystal (Fig. 1b) and measured by means of optical microscopy [27–29].

Most recent measurements were performed by in situ observations and recording of grain boundary migration in a SEM using a commercial hot deformation (tension-compression) stage<sup>1</sup> integrated in a SEM JEOL 820 and adapted to apply normal stresses to bicrystals with the respective geometry (Fig. 1a) at elevated temperatures up to  $850^\circ\text{C}$  [30]. Upon application of a constant load, i.e., a constant stress to the sample, the boundaries are displaced as can be observed and measured in situ utilizing the orientation contrast of the specimen surface revealed by an electron backscatter detector (Fig. 2) [30]. For characterization of the boundary migration-shear relation the surface of the specimens was scratched parallel to their axis prior to annealing to produce reference marks (Fig. 3). An analysis of the recorded orientation image sequences with a special software<sup>2</sup> reveals the normal boundary displacement  $d$  and the lateral grain translation  $s$  (Fig. 3), from which the migration rate  $v$  and shear  $\gamma=s/d$  can be determined.

## Experimental proof of the boundary migration-shear coupling

The response of planar tilt grain boundaries to an applied mechanical stress was investigated on bicrystalline specimens of high purity Al (99.998%) containing symmetrical  $\langle100\rangle$  tilt boundaries with 34 different misorientation angles in the range between 5 and  $85^\circ$ .

The experimental results confirmed that stress-driven grain boundary motion is coupled to a shear strain of the

<sup>1</sup> Kammrath & Weiss company.

<sup>2</sup> a4i Docu+IMES supplied by Aquinto company.

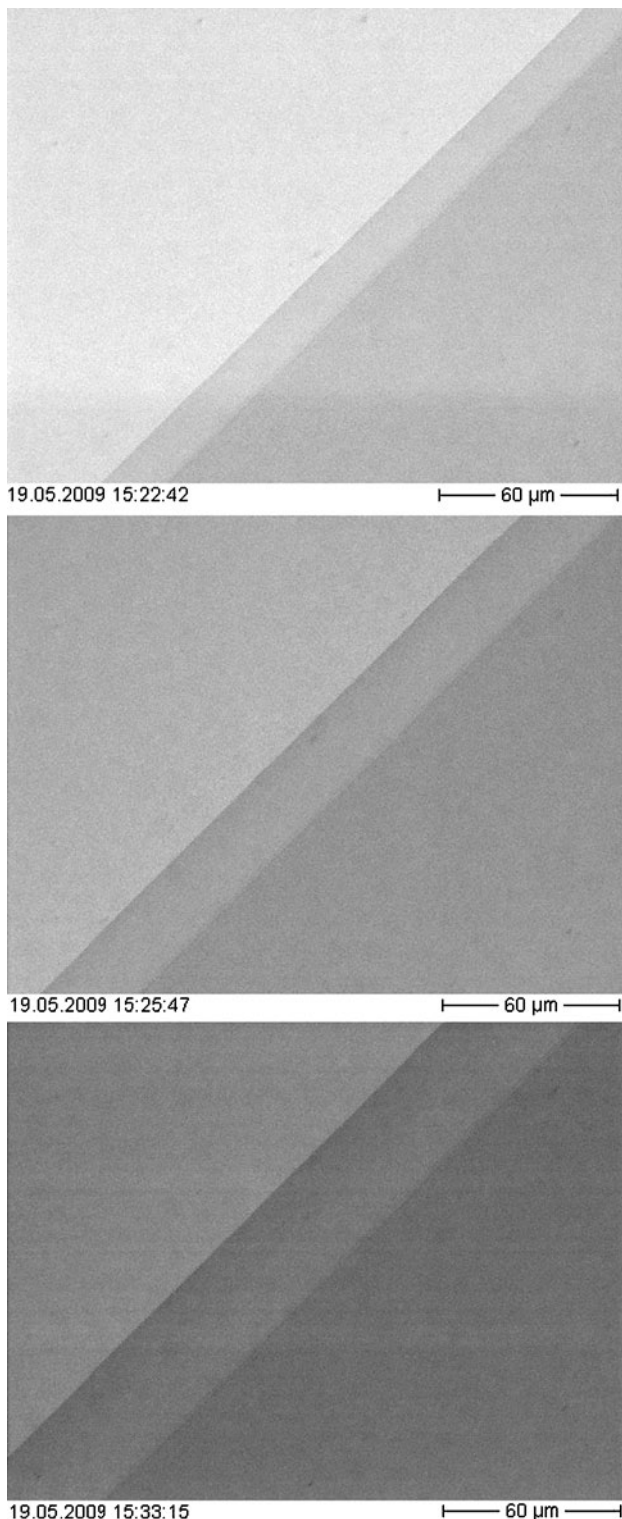


**Fig. 2** Migration of a  $76.4^\circ\langle 100 \rangle$  tilt grain boundary in Al bicrystal under an applied tensile stress of 0.26 MPa during annealing at  $380^\circ\text{C}$

crystal region behind the moving boundary. This is particularly apparent from marking lines on the surface of the bicrystals (Fig. 3).

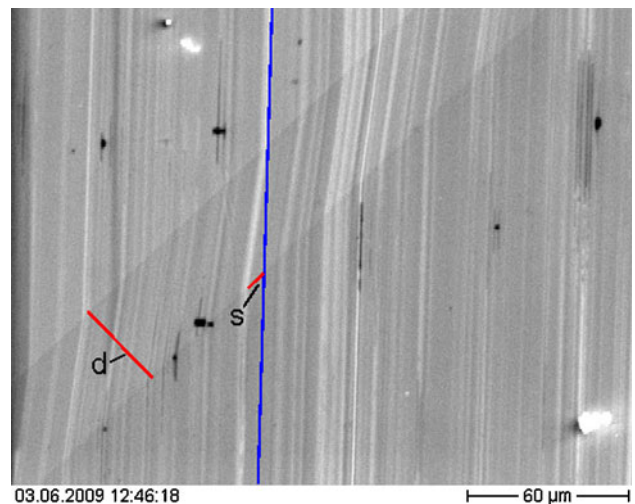


**Fig. 3** Coupling between grain boundary migration and shear strain is characterized by the factor  $\beta$ , which is defined as the ratio of the lateral grain translation  $s$  to the normal boundary displacement  $d$ ,  $\beta = \gamma = s/d$

Prior to the recent renewed interest in coupled grain boundary migration as a mechanism of nanocrystal plasticity and corresponding theoretical and simulation activities, the understanding of this phenomenon was based on the experimental results of bicrystal with low misorientation angle and very few high angle tilt boundaries [8–18]. According to this understanding [31], the coupled boundary motion is typical for low angle tilt boundaries, whereas in case of high angle boundaries in bicrystals subjected to a shear stress the strain remains basically localized in the boundary plane without boundary displacement normal to its plane (grain boundary sliding), and only for special high-angle boundaries with low  $\Sigma$  CSL relationships a normal migration coupled to shear can be observed and was attributed to the motion of secondary grain boundary dislocations [12–14].

Contrary to this understanding the measurements on Al bicrystals with various  $\langle 100 \rangle$  tilt boundaries revealed that the boundary migration-shear coupling is not confined to low angle and some special low  $\Sigma$  high-angle boundaries, but occurs also for non-coincidence high angle  $\langle 100 \rangle$  tilt boundaries [28, 29].

The coupling between boundary migration and shear strain can be characterized by the ratio of the grain translation  $s$  and the normal boundary displacement  $d$ ,  $\beta = \gamma = s/d$  (Fig. 3), which is referred to as the coupling factor [32].

As seen in Fig. 4, the values of the coupling factor experimentally obtained for the investigated  $\langle 100 \rangle$  tilt boundaries are in excellent agreement with the values calculated according to the geometrical model of coupled boundary migration [19, 20]. This model predicts that the coupling between shearing and migration can be observed

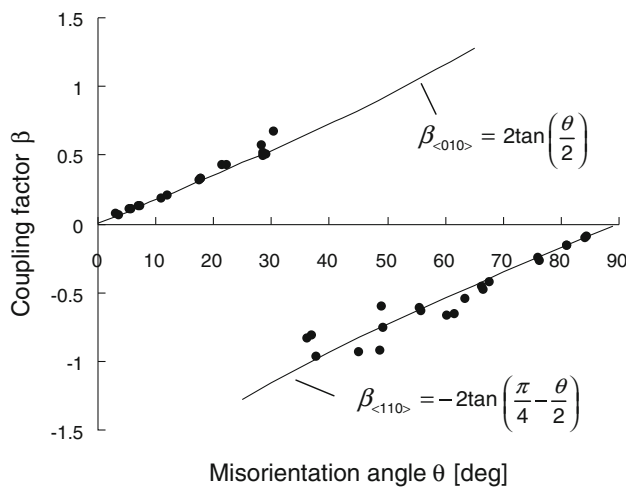


**Fig. 4** Misorientation dependence of measured (points) and calculated (lines) coupling factors for the investigated  $\langle 100 \rangle$  symmetrical tilt grain boundaries. The experimentally obtained values of the coupling factor were averaged over all specimens of the respective bicrystal

for any tilt boundary, no matter whether low- or high-angle. For  $\langle 100 \rangle$  tilt boundaries the coupling factor can be calculated as

$$\beta_{(010)} = 2 \tan\left(\frac{\theta}{2}\right) \text{ or } \beta_{(110)} = -2 \tan\left(\frac{\pi}{4} - \frac{\theta}{2}\right) \quad (1)$$

These expressions were initially derived for the motion of low angle tilt boundaries [7] that can formally be represented by slip of dislocations with Burgers vector  $\mathbf{b} = a\langle 010 \rangle$  on a  $\{001\}$  plane or  $\mathbf{b} = a/2\langle 110 \rangle$  on  $\{110\}$ , respectively. Therefore, the experimental results prove that for  $\langle 100 \rangle$  tilt boundaries there are indeed two geometrically different mechanisms ( $\langle 100 \rangle$  and  $\langle 110 \rangle$  modes as defined in [19, 20]) of coupling which switch at a misorientation angle between  $30.5^\circ$  and  $36.5^\circ$ . Furthermore, the results substantiate that although in high angle boundaries the structural dislocations can not be resolved, the Frank–Bilby equation [31] formally still applies.

### Boundary mobility, its temperature and misorientation dependence

Measurements performed at different elevated temperatures revealed that stress driven boundary migration is thermally activated and that its rate  $v_n$  depends on temperature according to an Arrhenius relation  $v_n = v_0 \exp(-H/kT)$ , where  $H$  is the activation enthalpy of grain boundary migration. The grain boundary mobility  $m$  for  $\langle 100 \rangle$  tilt boundaries was determined from the normal boundary velocity  $v_n$  and the driving force  $p$ :  $m = v_n/p$ . The driving force was calculated as  $p = \tau \sin \varphi$ , where  $\tau$

was the applied resolved shear stress and  $\varphi = \theta$  for misorientations close to 0, whereas  $\varphi = \theta - 90^\circ$  for  $\theta$  close to  $90^\circ$  [27].

Boundary motion was measured in the temperature range between 280 and 400 °C. The migration activation parameters ( $H$  and  $m_0 = v_0/p$ ) obtained from Arrhenius plots for all investigated boundaries are given in Fig. 5. As seen in Fig. 5, in both low angle regimes of the misorientation angle ( $\theta < 18^\circ$  and  $\theta > 76^\circ$ ) the measured activation enthalpy and the pre-exponential factor do not change essentially. The values of  $H$  vary only slightly around the mean value of about  $H = 1.45$  eV. By contrast, the high angle region is characterized by a specific misorientation dependence of the activation parameters, such that the lower  $H$  and  $m_0$  values correspond to boundaries with misorientations close to low  $\Sigma$  CSL-orientation relationships. Apparently, the migration mechanism for low angle boundaries remains essentially unaffected by a change of the tilt angle, whereas it can differ substantially for structurally different high angle boundaries.

It is worth noting that the migration activation enthalpies of  $\langle 100 \rangle$  tilt grain boundaries obtained in this experiment substantially differ from those obtained recently in our experiments with curvature driven  $\langle 100 \rangle$  tilt grain boundaries with misorientations between 15 and  $45^\circ$  in bicrystals of high purity Al [33, 34]. The activation enthalpies for curvature driven boundaries were in the range between 1.7 and 2.8 eV that is much higher than the activation enthalpy measured for stress driven boundaries (Fig. 6). This difference in the migration activation enthalpy for differently driven boundaries strongly indicates that the migration mechanisms may depend on the kind of driving force for boundary motion and its coupling with the boundary structure.

### Experimental observation of the boundary migration-shear coupling for asymmetrical tilt boundaries

As has been reported in previous sections, the stress induced migration of any symmetrical  $\langle 100 \rangle$  tilt boundary in Al is associated with a shear strain of the bicrystal and the relation between normal boundary displacement and tangential grain translation follows the tangent rule (Eq. (1)). However, most grain boundaries in a real polycrystal are asymmetrical. Therefore, the response of some asymmetrical boundaries to an applied stress was addressed in this study.

The structure of asymmetrical  $\langle 100 \rangle$  tilt boundaries consists of mixed arrangement of dislocations with both  $a\langle 010 \rangle$  and  $a/2\langle 110 \rangle$  Burgers vectors, which under the applied stress should move in different planes. For symmetrical low-angle boundaries with misorientations close

**Fig. 5** Activation parameters (activation enthalpy  $H$  and pre-exponential mobility factor  $m_0$ ) of stress-induced migration of  $\langle 100 \rangle$  symmetrical tilt grain boundaries

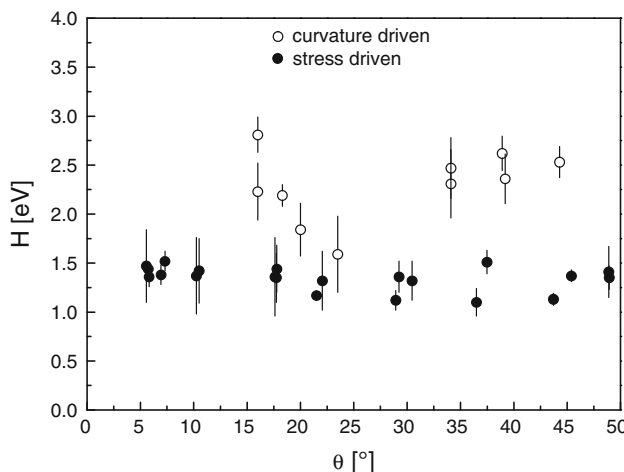
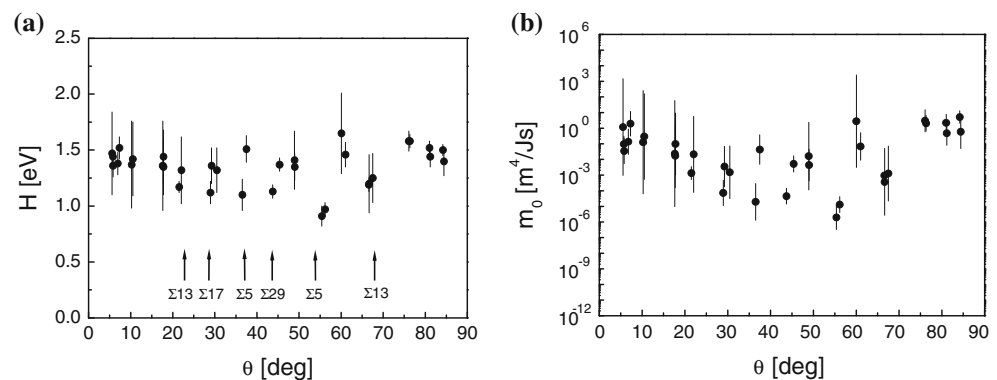


**Fig. 6** Comparison of the activation enthalpies for stress driven (solid symbols) and curvature driven migration [33, 34] of  $\langle 100 \rangle$  tilt boundaries in commercially pure (99.998%) and high purity (99.9995%) Al, respectively

to  $0^\circ$  and  $90^\circ$  dislocations of each type can glide on different slip planes and the corresponding grain boundaries move in opposite directions in response to the same shear stress. In case of asymmetrical boundaries it seems that the dislocations with different Burgers vectors gliding on intersecting slip planes cannot move together without hindering and locking each other. Therefore, according to Read and Shockley the motion of the asymmetrical (low angle) boundaries under stress and, consequently, the lateral translation of adjacent grains are impossible [7]. By contrast, recent models do not impose any restrictions on asymmetrical boundaries. In particular, the model by Cahn et al. [19, 20] predicts that the coupling factor only depends on the tilt angle but not on the boundary plane inclination. Also, the model by Caillard et al. [21, 22] describes the shear-migration coupling for any boundary, no matter whether symmetrical or asymmetrical.

The experimental results revealed that asymmetrical  $\langle 100 \rangle$  tilt boundaries move under an applied stress and that this motion is accompanied by a shape change of the bicrystal, but the obtained coupling factors distinctly

deviate from the coupling factor calculated according to the tangent rule. Figure 7 depicts an example of such behavior for an asymmetrical  $17.4^\circ\langle 100 \rangle$  boundary with a  $19.1^\circ$  inclination of the boundary plane from the symmetrical orientation.

Therefore, contrary to the expectations based on the dislocation model of grain boundaries [7], the experiments proved that the asymmetrical tilt boundaries can move under an applied stress and produce a shear. Further investigations, especially molecular dynamics simulations are obviously needed to clarify the mechanisms of this phenomenon, specific atomic rearrangements, dislocation processes, and reactions involved in the process of boundary migration.

#### Effect of material purity on boundary migration under stress

It is textbook knowledge that solutes in solids reduce the rate of grain boundary motion. The dependence of the migration parameters upon impurity concentration for curvature driven boundaries in aluminum bicrystals was determined in [35, 36]. In this study the impact of solute atoms on stress-driven boundary motion coupled to shear was addressed. The experiments were carried out on bicrystals produced from aluminum of different production and purity, 99.9999, 99.9995, and 99.998%. The migration of symmetrical  $9.8, 10.5, 11.0$ , and  $11.2^\circ\langle 100 \rangle$  tilt boundaries under an applied stress was measured. Since the tilt angles of the investigated boundaries were very close to each other and the migration parameters for the  $\langle 100 \rangle$  boundaries in aluminum of equal purity practically did not change up to a tilt angle of  $18^\circ$  (Fig. 5), the mobility data obtained in the current measurements were considered to be relevant for  $\langle 100 \rangle$  boundaries with an average tilt angle of  $10.5^\circ$ .

Figure 8a depicts the temperature dependence of the boundary mobility in aluminum of different purity. As seen, the boundary mobility decreased with increasing

**Fig. 7** **a** Geometry of a bicrystal with an asymmetrical  $17.4^\circ\langle 100 \rangle$  boundary with  $19.1^\circ$  inclination from the symmetrical position; **b** optical image of the bicrystal surface showing boundary migration-shear coupling,  $\beta = 0.39$  ( $\beta_{\text{theor}} = 0.31$ )

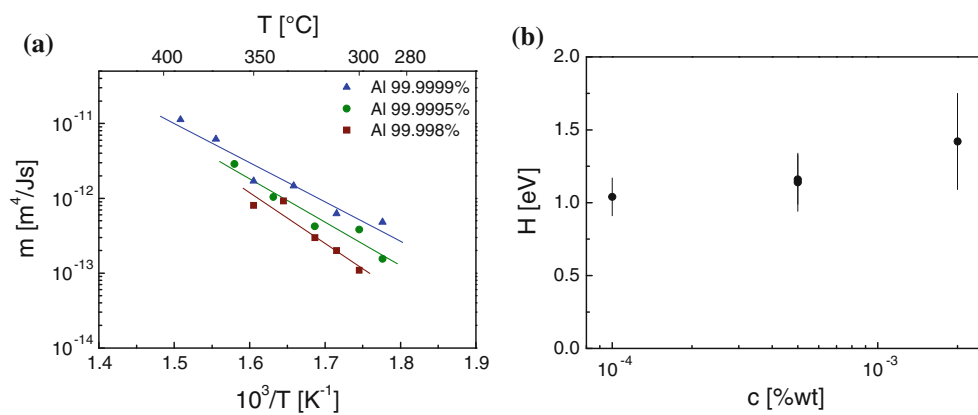
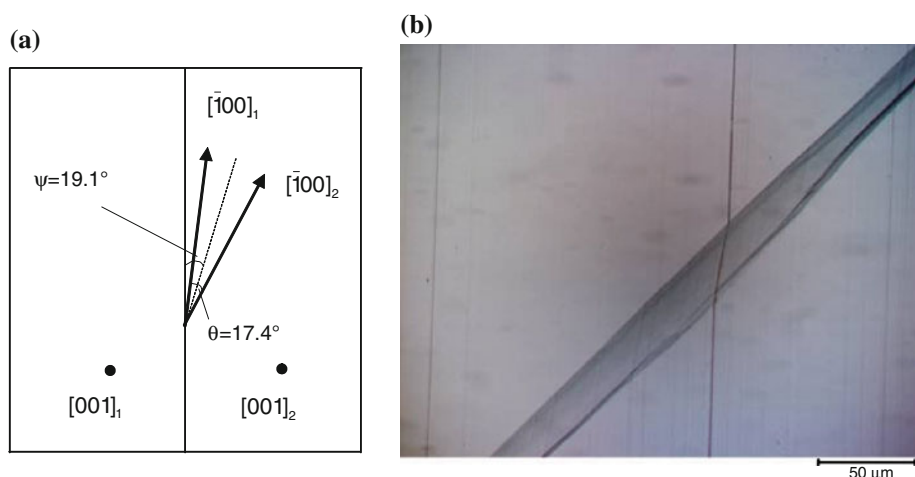


**Fig. 8** Temperature dependence of the mobility for  $10.5^\circ\langle 100 \rangle$  tilt boundary in Al of different purity. **a** Arrhenius plots. **b** migration activation enthalpy versus impurity concentration

impurity content. The migration activation enthalpy obtained from the corresponding Arrhenius plots rises from 1.04 eV in Al with  $10^{-4}\%$  solute content up to 1.37 eV in Al with  $2 \times 10^{-3}\%$  impurities (Fig. 8b). The pre-exponential factor behaves similarly, increasing over the investigated range of solute content by more than two orders of magnitude from  $7.2 \times 10^{-4}$  to  $2.9 \times 10^{-1} \text{ m}^4/\text{J s}$ .

The impact of impurities on grain-boundary motion was considered in the frame of the impurity drag theory [37–39]. The theory predicts that the activation enthalpy is independent of impurity concentration and that the pre-exponential factor decreases with increasing solute content in a hyperbolic fashion. Both predictions did not agree with the results of the current measurements of stress-induced boundary migration.

It is worth noting that a similar although slighter increase of the activation enthalpy with rising impurity concentration was observed in experiments with curved boundaries moving under a capillary driving force [36]. The pre-exponential mobility factor for curvature driven

boundary migration, however, remained essentially unchanged with increasing impurity concentration.

The reduction of the boundary migration rate due to an increase of the activation enthalpy in this experiment suggests that impurity atoms substantially affect the migration mechanism. Apparently, a higher solute segregation causes a higher migration activation enthalpy, i.e., to a great extent defines the rearrangement of atoms between the crystals to another during boundary displacement. Molecular dynamics simulations [20] revealed that migration of  $\langle 100 \rangle$  tilt boundaries under stress proceeds by a rearrangement of atomic lattice sites (atomic shuffling), which does not require “classical” bulk diffusion. However, the measured activation enthalpy can be attributed to a diffusion of the impurity atoms segregated to the boundary in a real bicrystal.

As reported above, for stress-induced grain boundary motion there is a misorientation dependence of migration activation enthalpy (Fig. 5). The lower H values were measured for boundaries with misorientations close to low  $\Sigma$  CSL orientation relationships. By contrast, the activation

enthalpy for grain boundary diffusion is known to be maximal for low  $\Sigma$  tilt boundaries and decreases with deviation from the coincidence misorientation [40, 41]. However, a diffusion of segregated impurities with a moving boundary must not be necessarily associated with a diffusion along the boundary measured in experiments [40, 41], but with the atomic transfer within the boundary in the direction normal to the boundary plane. This process can be expected to be more close to bulk diffusion than to diffusion along the boundary. The segregation behavior of low  $\Sigma$  tilt boundaries can be expected to differ from that of non-coincidence boundaries, which is reflected in their lower migration activation enthalpy.

On the other hand, lower solutes segregation in a material of higher purity may result in a less disturbed/changed boundary structure that, in turn, makes a diffusion of impurity atoms in the boundary region easier and leads to the lower activation enthalpy of boundary migration as observed in the experiment (Fig. 8).

### Formation and growth of sub-grains during stress-driven boundary migration

The experimental observations also revealed that coupled boundary motion under stress can be accompanied by the

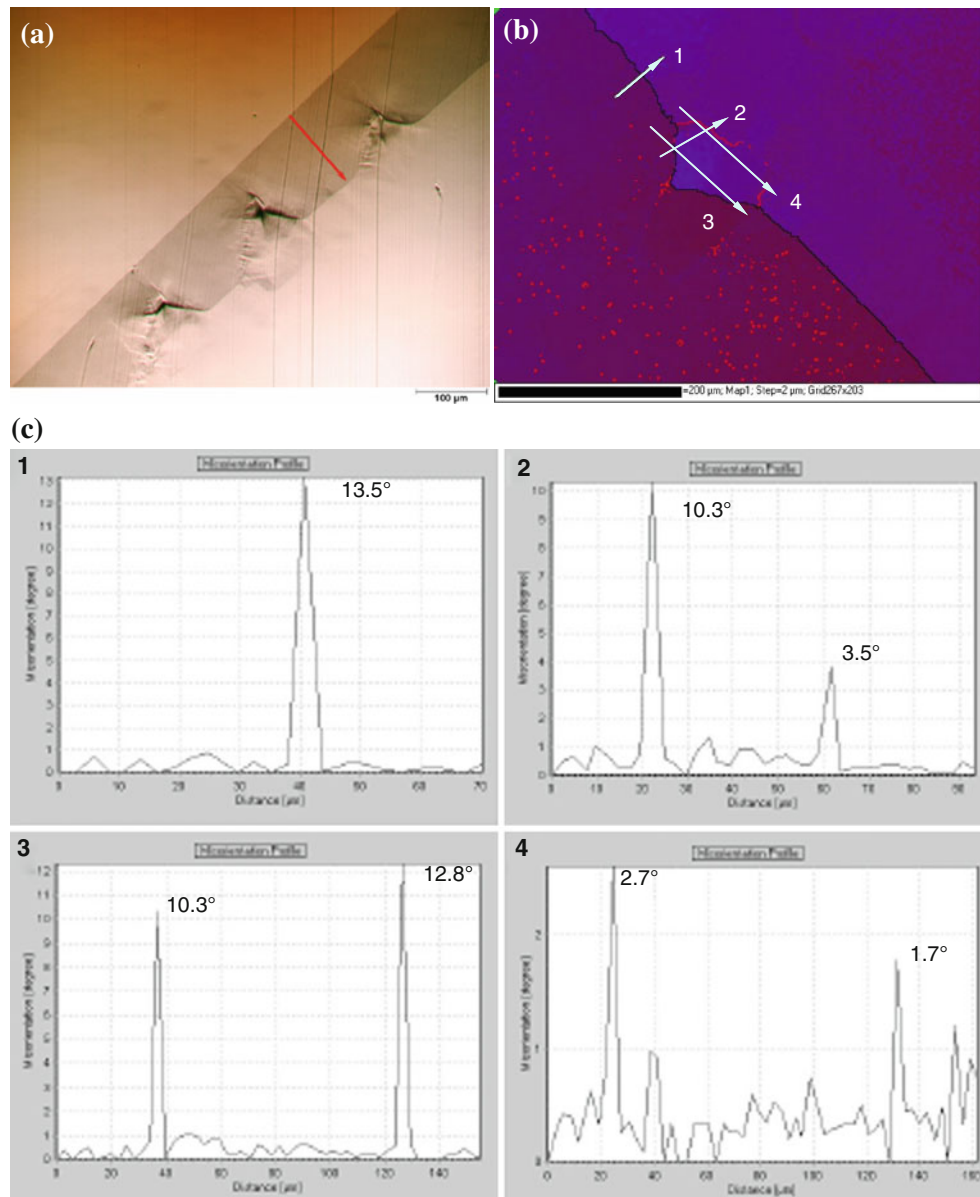


**Fig. 9** Generation and growth of new grains during migration of a 76.3°(100) tilt grain boundary. **a** optical micrograph after annealing at 370 °C for 60 min under a tensile stress of 0.84 MPa. **b** single newly

formed grain and **c** change of orientation across its boundaries as obtained by EBSD measurements

formation of new grains disoriented with respect to both original grains of the bicrystal (Fig. 9). These grains are generated at the boundary, can possess an orientation gradient and grow by following the moving boundary in the direction of the consumed grain. Their formation and growth was associated with the appearance of various folds on the surface of the sample (Fig. 9), which accommodate arising plastic incompatibilities. Usually, starting from one location at the initial boundary these grains develop into groups of sub-grains separated from each other and the original consumed grain of the bicrystal by low-angle boundaries. The boundaries between sub-grains and the growing grain remain stable and with progressing migration of the original grain boundary the sub-grains become wider (Fig. 9). This can eventually result in the transformation of the extended boundary sections into a band with polycrystalline sub-grain structure. The described behavior during stress driven boundary migration was observed for  $\langle 100 \rangle$  tilt boundaries with any misorientation angle, but more often for high-angle boundaries. Orientation measurements by serial sectioning EBSD revealed that the size of newly formed grains in the direction normal to the surface was comparable to their size on the surface.

It is well established that grain boundaries and triple junctions can act as effective sources of lattice dislocations under an applied stress during plastic deformation [31]. Computational investigations [42, 43] have shown that at low temperatures where grain boundaries remain stable, stress concentrations caused by the elastic anisotropy of adjacent grains or by steps on the boundary plane are of minor importance with regard to dislocation generation in metallic materials. However, during grain boundary sliding at elevated temperatures the existence of a step on a boundary can lead to very high stress concentrations of about  $G/35$  ( $G$ —shear modulus) that is close to the theoretical shear stress for dislocation nucleation ( $G/30$ ) [44, 45].

Apparently, the formation of new grains observed in this experiment is facilitated by the nucleation of a sufficient number of lattice dislocations by the grain boundary during its stress-driven migration coupled to shear deformation. Then, these dislocations build walls and finally turn into sessile boundaries between the new grain and the growing grain of the original bicrystal and the moving low-angle boundary that separates the new grain from the consumed grain of the original bicrystal (Fig. 9).

An analysis of available experimental observations in Fe-3%Si, stainless steels and copper showed [45] that grain boundary dislocation sources can operate at applied shear stresses as low as  $G/1000$  to  $G/400$ . It can be concluded from these observations that stress-driven grain boundary in high purity aluminum can act as a source of dislocations even at much lower applied shear stresses of about  $G/60000$ .

## Summary

The shear stress-induced migration of planar symmetrical  $\langle 100 \rangle$  tilt boundaries with tilt angles in the entire misorientation range ( $0^\circ$  to  $90^\circ$ ) in aluminum bicrystals was observed to be coupled to a lateral translation of the adjacent grains. This coupling proved to be the typical migration mode of any  $\langle 100 \rangle$  tilt boundary, no matter whether low- or high-angle, low  $\Sigma$  CSL coincidence or non-coincidence boundary. The measured ratios of the normal boundary motion to the tangential displacement of the grains were in an excellent agreement with theoretical predictions.

For stress-induced grain boundary motion there is a misorientation dependence of the migration activation parameters. The lower values of the activation enthalpy and the pre-exponential mobility factor can be associated with boundaries with tilt angles close to low  $\Sigma$  CSL-orientation relationships.

The results revealed that the coupling between normal boundary migration and shear is not confined to symmetrical tilt boundaries only, but also asymmetrical boundaries are capable to move under an applied stress and produce shear.

The measurements of the coupled boundary migration in aluminum of different purity revealed that impurities retard boundary motion. Both the migration activation enthalpy and the pre-exponential mobility factor increase with rising impurity concentration. This observation cannot be accounted for by the theory of impurity drag of boundary migration.

The experimental observations provide evidence that the investigated boundaries can act during their coupled migration under stress as sources of lattice dislocations that results in the formation and growth of new grains in the boundary region.

**Acknowledgements** The authors express their gratitude to the Deutsche Forschungsgemeinschaft for financial support (Grant MO 848/10-2).

## References

- Haslam A, Moldovan D, Yamakov V, Wolf D, Phillpot S, Gleiter H (2003) Acta Mater 51:2112
- Farkas D, Frøseth A, Van Swygenhoven H (2006) Scripta Mater 55:695
- Gianola GS, Van Petegem S, Legros M, Brandstetter S, Van Swygenhoven H, Hemker KJ (2006) Acta Mater 54:2253
- Legros M, Gianola GS, Hemker KJ (2008) Acta Mater 56:3380
- Rupert TJ, Gianola DS, Gan Y, Hemker KJ (2009) Science 326:1686
- Mompiou F, Caillard D, Legros M (2009) Acta Mater 57:2198
- Read WT, Shockley W (1950) Phys Rev 78:275
- Washburn J, Parker ER (1952) Trans AIME 194:1076

9. Li CH, Edwards EH, Washburn J, Parker ER (1953) *Acta Metall* 1:223
10. Bainbridge DW, Li CH, Edwards EH (1954) *Acta Metall* 2:322
11. Watanabe T, Kimura SI, Karashima S (1984) *Philos Mag A* 49:845
12. Horiuchi R, Fukutomi H, Takahashi T (1987) In: Ishida Y (ed) Fundamentals of diffusion bonding. Elsevier, Amsterdam, p 347
13. Fukutomi H, Kamiyo T (1985) *Scripta Metall* 19:195
14. Fukutomi H, Iseki T, Endo T, Kamiyo T (1991) *Acta Metall Mater* 39:1445
15. Sheikh-Ali AD, Valiev RZ (1990) *Phys Status Solidi (a)* 117:429
16. Sheikh-Ali AD, Lavrentyev FF, YuG Kazarov (1997) *Acta Mater* 45:4505
17. Sheikh-Ali AD, Szpunar JA (1998) *Mater Sci Eng A* 245:49
18. Yoshida H, Yokoyama K, Shibata N, Ikuhara Y, Sakuma T (2004) *Acta Mater* 52:2349
19. Cahn JW, Mishin Y, Suzuki A (2006) *Philos Mag* 86:3965
20. Cahn JW, Mishin Y, Suzuki A (2006) *Acta Mater* 54:4953
21. Caillard D, Mompou F, Legros M (2009) *Acta Mater* 57:2390
22. Mompou F, Legros M, Caillard D (2010) *Acta Mater* 58:3676
23. Suzuki A, Mishin Y (2005) *Mater Sci Forum* 502:157
24. Ivanov VA, Mishin Y (2008) *Phys Rev B* 78:064106
25. Zhang H, Du D, Srolovitz DJ (2008) *Philos Mag* 88:243
26. Elsener A, Politano O, Derlet PM, Van Swygenhoven H (2009) *Acta Mater* 57:1988
27. Molodov DA, Ivanov VA, Gottstein G (2007) *Acta Mater* 55:1843
28. Molodov DA, Gorkaya T, Gottstein G (2007) *Mater Sci Forum* 558–559:927
29. Gorkaya T, Molodov DA, Gottstein G (2009) *Acta Mater* 57:5396
30. Gorkaya T, Burlet T, Molodov DA, Gottstein G (2010) *Scripta Mater* 63:633
31. Sutton AP, Balluffi RW (1995) Interfaces in crystalline materials. Clarendon, Oxford
32. Cahn JW, Taylor JE (2004) *Acta Mater* 52:4887
33. Kirch DM (2008) In Situ SEM investigation of individual and connected grain boundaries in aluminum. Cuvillier Verlag, Göttingen
34. Kirch DM, Jannot E, Barrales-Mora LA, Molodov DA, Gottstein G (2008) *Acta Mater* 56:4998
35. Gottstein G, Molodov DA, Czubayko U, Shvindlerman LS (1995) *J de Phys IV* 5:89
36. Molodov DA, Czubayko U, Gottstein G, Shvindlerman LS (1998) *Acta Mater* 46:553
37. Lücke K, Detert K (1957) *Acta Metall* 5:628
38. Cahn JW (1962) *Acta Metall* 10:789
39. Lücke K, Stüwe H (1963) In: Himmel L (ed) Recovery and recrystallization of metals. Interscience, New York, p 131
40. Surholt T, Molodov DA, Chr Herzig (1998) *Acta Mater* 46:5345
41. Aleshin AN, Faulkner RG, Molodov DA, Shvindlerman LS (2002) *Interface Sci* 10:5
42. Kurzydlowski K, Celinski Z, Grabski MM (1980) *Res Mech* 1:283
43. Celinski Z, Kurzydlowski K (1982) *Res Mech* 5:89
44. Hirth JP, Lothe J (1982) Theory of dislocations. Wiley, New York
45. Varin RA, Kurzydlowski K, Tangri K (1987) *Mater Sci Eng* 85:115